

Model for Spontaneous Frequency Sweeping of an Alfvén Wave in a Toroidal Plasma

G. Wang and H. L. Berk

Institute of Fusion Studies, University of Texas at Austin

TTF 2011

April 8, 2011, San Diego, CA

Outline

- Observations of TAE chirping events
- TAE chirping frequencies significantly different from that of linear mode
- Phase space structures of energetic particles in Alfvén gap and continuum
- Verification of understanding from the filtered response

TAE Wave Structure

- In a torus, wave solutions are quantized poloidally & toroidally:

$$\Phi(r, \theta, \zeta, t) \propto \exp(-i\omega t) \sum_m \Phi_m(r) \exp(im\theta - in\zeta)$$

- Parallel wave number k_{\parallel} determined by B-line twist $q(r) = rB_T / RB_p$ (“safety factor”):

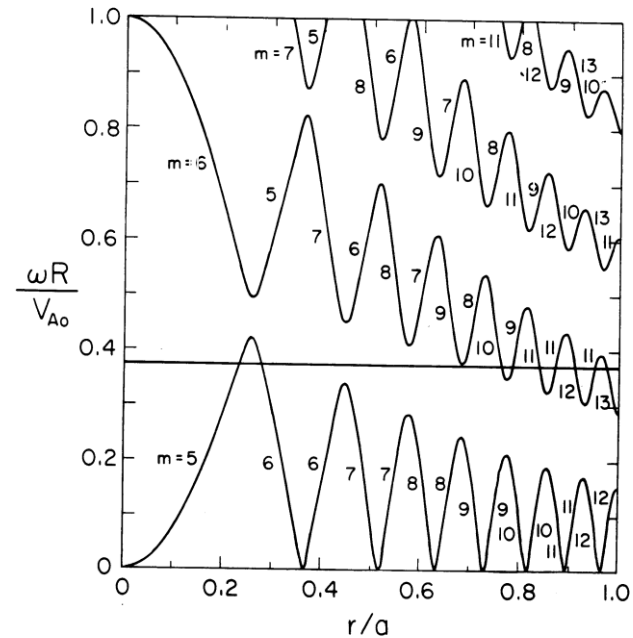
$$k_P(r) = \frac{1}{R} \left(\frac{m}{q(r)} - n \right)$$

- “Gaps” occur in Alfvén continuum in toroidal geometry when

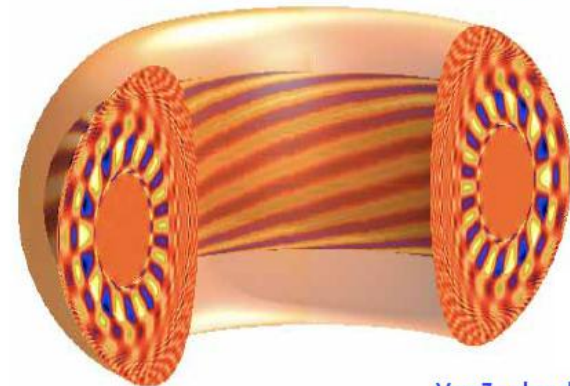
$$\omega = k_{Pm}(r) v_A(r) = -k_{Pm+1}(r) v_A(r)$$

Counter-propagating waves cause frequency gap

- Coupling avoids frequency crossing (waves mixing)
- Crossing occur at many position along the minor radius.



Calculated Alfvén Eigenmode structure in ITER

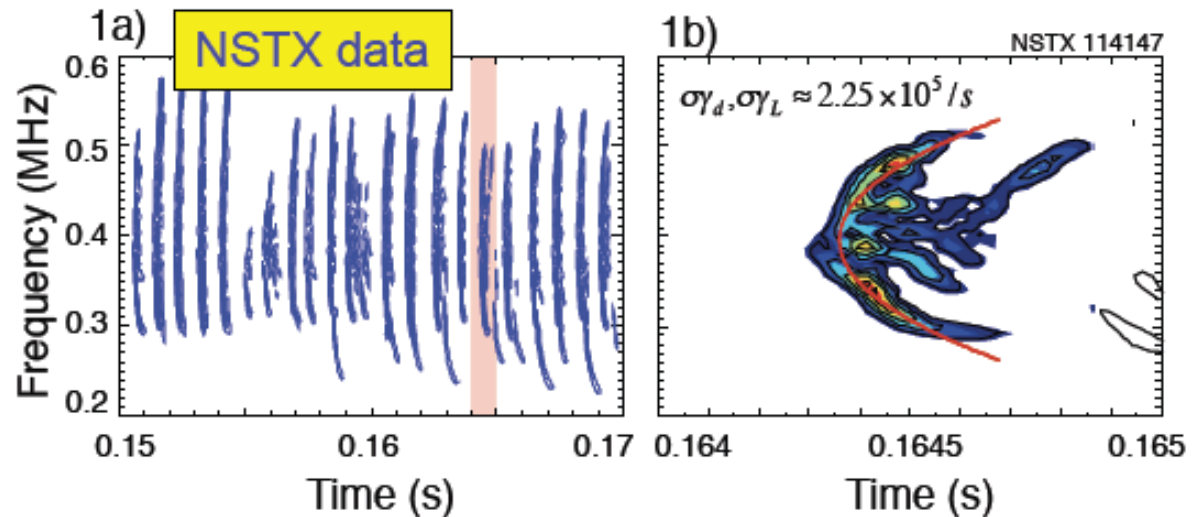


Berk-Breizman Model

- The analysis of nonlinear saturation for a single BGK mode was discussed by Berk and Breizman. The model treats the particles trapped in the potential well in the adiabatic approximation and obtained the saturation of wave amplitude and the frequency shift during the initial nonlinear stage.

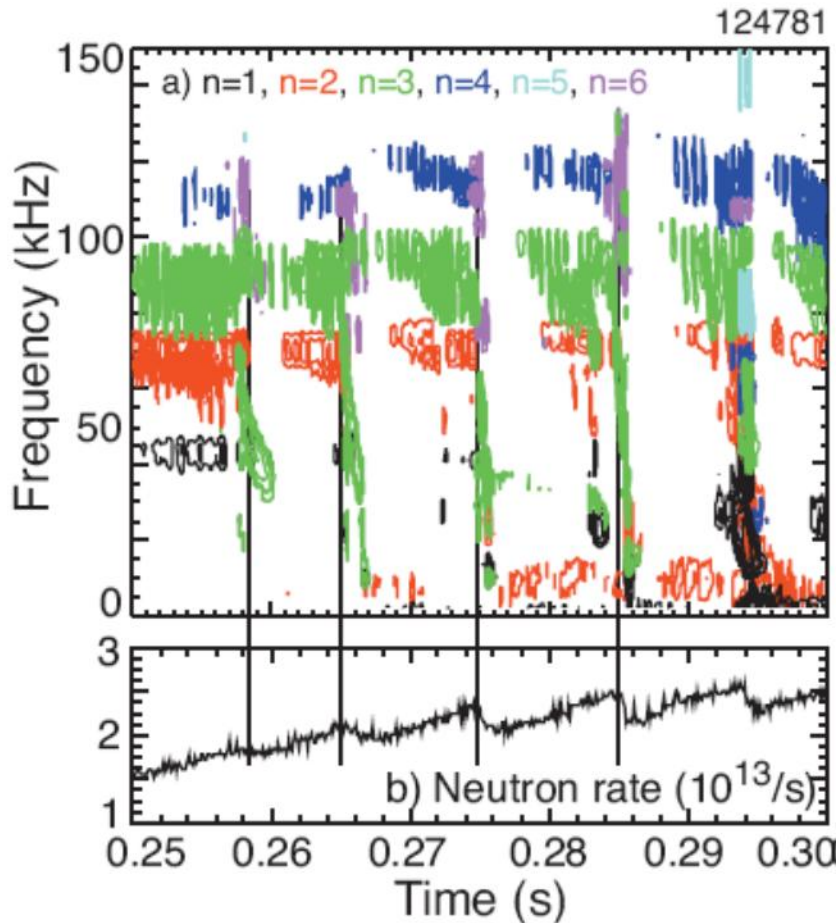
$$\frac{\omega_b}{\gamma_L} \approx \frac{16}{3\pi^2},$$

$$\frac{\delta\omega}{\gamma_L} \approx \frac{16}{3\pi^2} \sqrt{\frac{2}{3}} (\gamma_d t)^{1/2}.$$



- The ms timescale of these events is much shorter than the frequency variation of equilibrium profile [such a $q(\psi)$] confinement time in the plasma.
- Emerging frequency shifts vary with the square root of time, compatible with predictions of Berk-Breizman model.

Strong Frequency Chirping



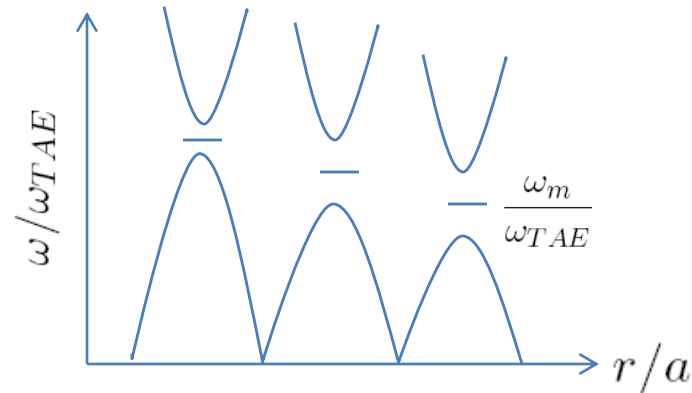
Recent TAE avalanche experiments in NSTX show spectrogram of magnetic fluctuations with each burst,

- The total TAE amplitude increases by roughly an order of magnitude.
- The dominant modes show strong downward frequency chirps.

Our work explores TAE fast chirping which involves spontaneous formation of nonlinear phase-space structures (holes and clumps).

- E.D.Fredrickson, et al. Phys. Plasmas 16(2009) 122505.
- M.Podesta, et, Phys. Plasmas 16(2009)056104.

Rosenbluth, Berk, VanDam (RBV) Tip Model



- RBV model connects inner region ‘jumps’ through tips to outer region jumps due to cylindrical solutions between tips.
- Inner region solutions have a relatively simple frequency dependence that can be inverted into the time domain.
- Dynamics of system can be expressed in variation form with the dependence due to the local ‘fluxes’ $C_m^\pm(r_m)$

Berk Mett Quadratic Form for RBV Model

$$\int_{-\infty}^{\infty} dh \left\{ \sum_m \frac{\pi^2 R_0 c^2 q'_m r_m n}{q_m^2 \omega_m} \begin{bmatrix} C_{m+1}^- \tilde{C}_{m+1}^- (\bar{\Delta}_{m+1}^- + \alpha_{m+1}^-) \\ + C_m^+ \tilde{C}_m^+ (\bar{\Delta}_m^+ + \alpha_m^+) \\ + \beta_{m+1}^- \tilde{C}_m^+ C_{m+1}^- \\ + \beta_m^+ \tilde{C}_{m+1}^- C_m^+ \\ - \tilde{\Delta}_{m+1}^+ \tilde{C}_{m+1}^+ C_{m+1}^- \\ - \tilde{\Delta}_m^- C_m^+ \tilde{C}_m^- \end{bmatrix} + i \sum_m \int_{(m)} d^3 r \tilde{\mathbf{E}} \cdot \delta \mathbf{j} \right\} \quad h_m = \frac{\omega_m - \omega_{m0}}{\epsilon \omega_{m0}}$$

$$\alpha_m = \frac{-(h - h_m)}{[1 - (h - h_m)^2]^{1/2}} \equiv \text{self component inner solution jump}$$

$$\beta_m = -\frac{1}{[1 - (h - h_m)^2]^{1/2}} \equiv \text{coupled component inner solution jump}$$

$\bar{\Delta}_m \equiv$ self component outer solution jump, $\tilde{\Delta}_m \equiv$ coupled component outer solution jump

1. δj is current due to energetic particles expressed in terms of the inner and outer solutions and proportional to the C's
2. Variation with respect to C_m^\pm gives equations in normalized frequency domain and in terms of energetic particle currents
3. Fourier transform to the time domain possible and produces couple set of integral equation for time evolution

Euler Equation in Time Domain

$$(\Delta_{m+1}-i)C_{m+1}(t)-i \int_0^t d\tau J_1(\tau)C_{m+1}(t-\tau)+ \int_0^t d\tau J_0(\tau)C_m(t-\tau) = \hat{S}_{11}C_{m+1}+\hat{S}_{12}C_m$$

$$(\Delta_m-i)C_m(t)+ \int_0^t d\tau J_0(\tau)C_{m+1}(t-\tau)-i \int_0^t d\tau J_1(\tau)C_m(t-\tau) = \hat{S}_{21}C_{m+1}+\hat{S}_{22}C_m$$

Simplified equation for a single symmetric couplet and we simplify the of model energetic particle interaction (work in progress for more systematic model)

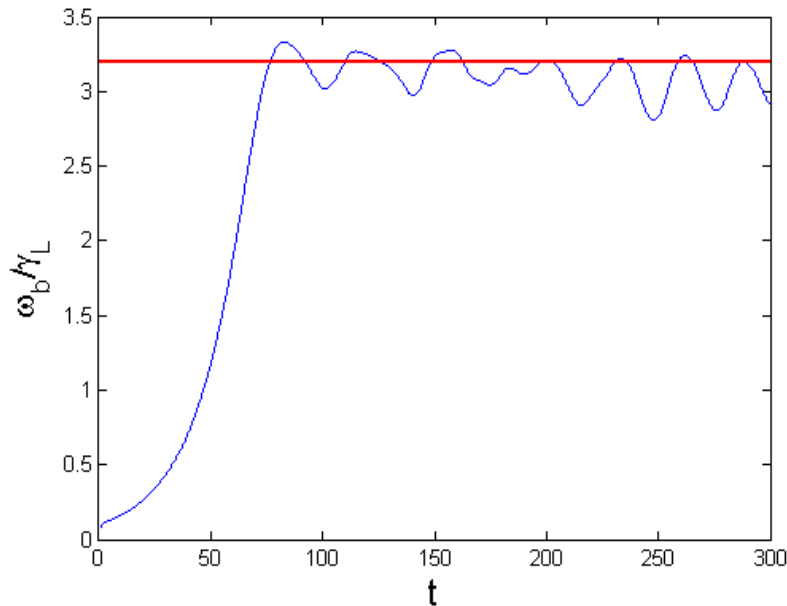
The time integral wave equation : $A(t) = C_m(t) + C_{m+1}(t)$

$$A(t) = \frac{1}{\Delta_m - i} \int_0^t (J_0(t-\tau) - iJ_1(t-\tau)) e^{-\gamma_d(t-\tau)} A(\tau) d\tau - \frac{2i\eta_m}{\Delta_m - i} \int_{-\infty}^{\infty} f_{k_1=1}(\Omega, t) d\Omega.$$

Combined with the Vlasov equation in a single mode case,

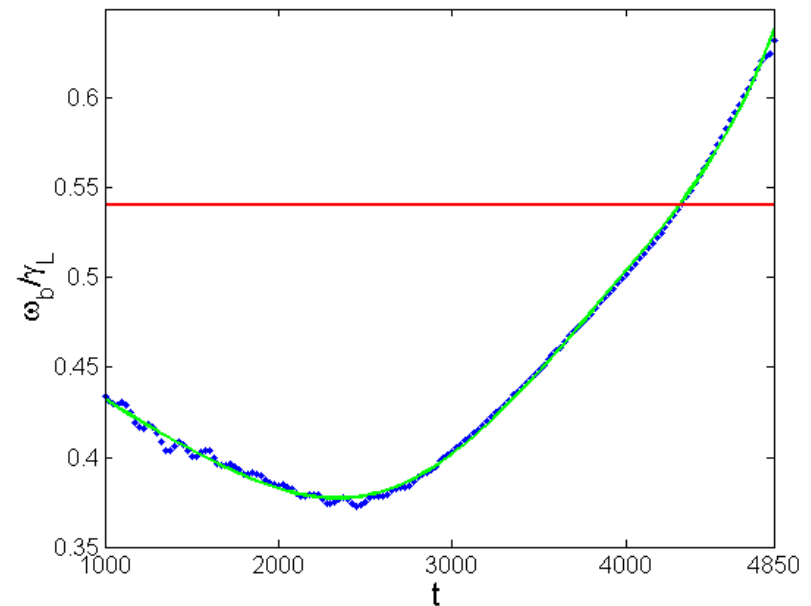
$$\frac{\partial f}{\partial t} + \Omega \frac{\partial f}{\partial \theta} - \text{Re}\{A(t)e^{i\theta}\} \frac{\partial f}{\partial \Omega} = 0.$$

The Bifurcation of Saturation Level



Without the damping, the saturation level:

$$\frac{\omega_b}{\gamma_L} \simeq 3.2$$



The saturation level with damping:

$$\gamma = \gamma_L - \gamma_d = 0.2\gamma_L \quad (\gamma_L = 0.1)$$

$$\frac{\omega_b}{\gamma_L} \simeq \frac{16}{3\pi^2}$$

The Chirping Mode is Tracked

- The oscillation frequency of the chirping impairs the numerical accuracy of the simulation as the chirping evolves and develops.
- The tracking method is developed to calculate the wave/particle dynamics in a calculation frame

$$a(t) = A(t)e^{i(\theta-\theta_0)}, \tilde{f}_n = \tilde{F}_n e^{in(\theta-\theta_0)-is(\Omega-\Omega_0)}$$

that is nearly the same as the velocity of the phase space structure being tracked.

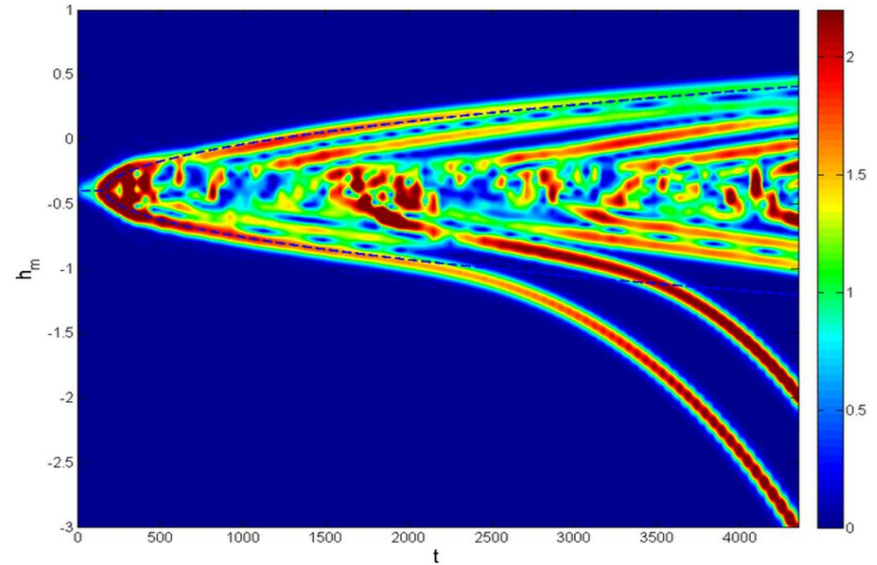
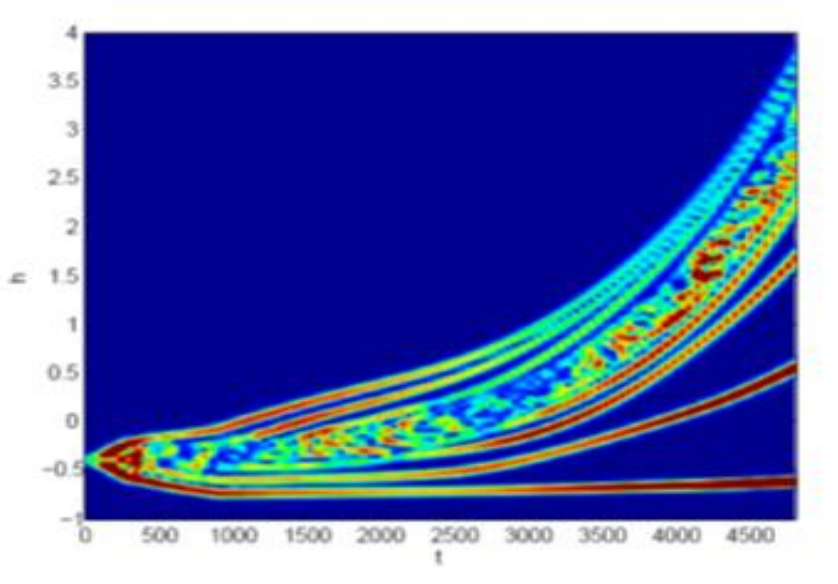
- The motion of the calculation frame is governed by

$$\frac{d\theta(t)}{dt} = h_{rex}(t) + i\gamma d.$$

$$\frac{dh_{rex}(t)}{dt} = \frac{h(T) - h_{rex}(t)}{\tau}$$

where the “velocity” of the calculation frame h_{rex} is the same as the frequency of the tracking chirping signal.

Spectrogram of TAE Signals



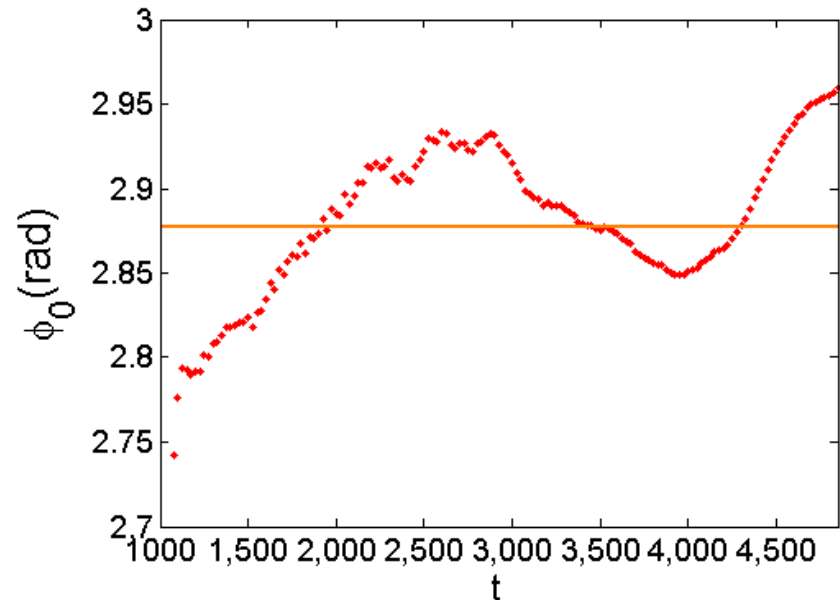
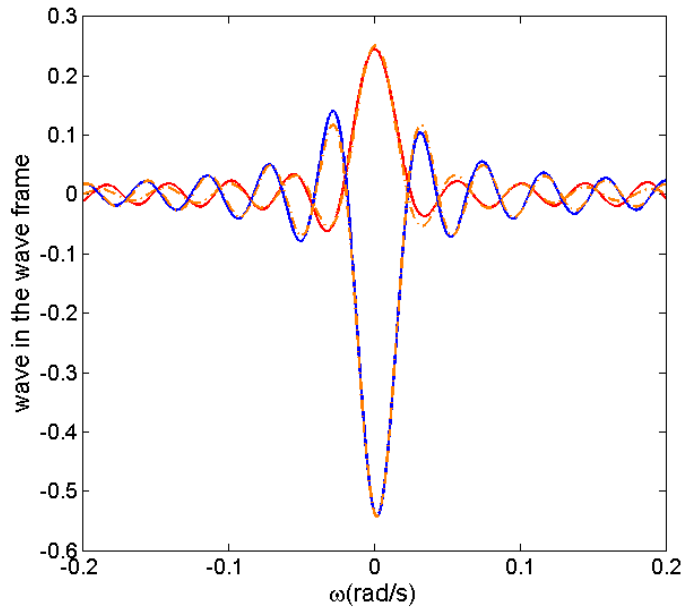
- The initial chirping spectrum chirps in accord with the frequency shift varying with the square root of time.

$$\frac{\delta\omega}{\gamma_L} \simeq \frac{16}{3\pi^2} \sqrt{\frac{2}{3}} \gamma_d t$$

- The robust chirping branch separates from the linearly predicted frequency and approaches the gap-continuum boundary.

Chirping Filter

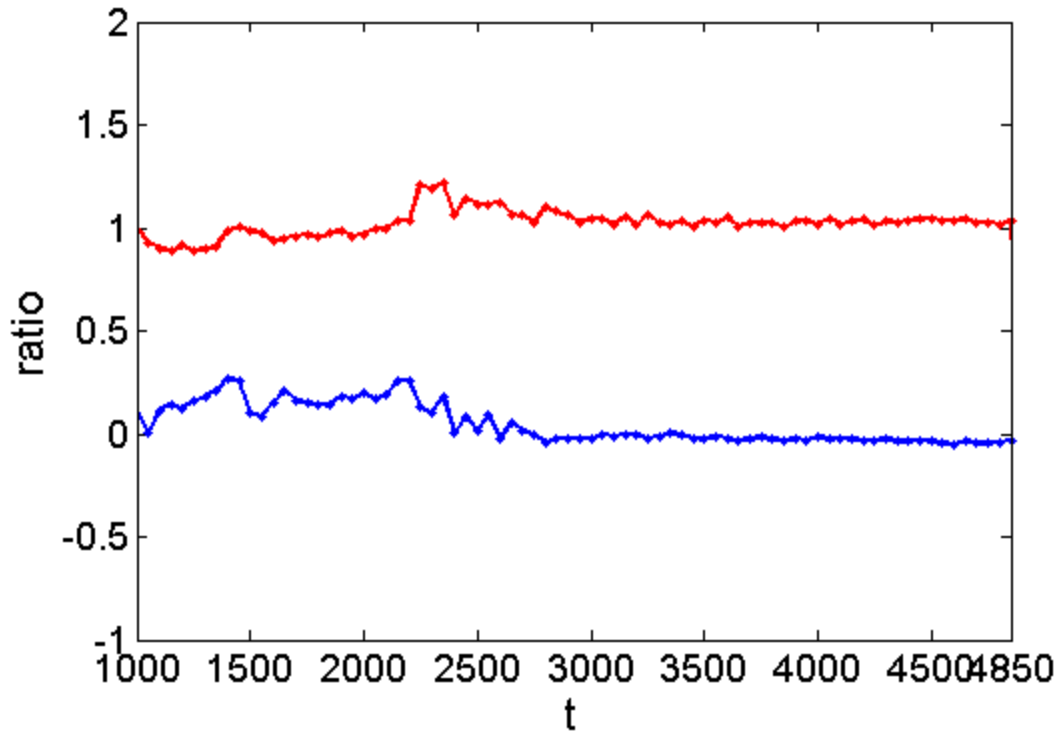
- The expected signal is chirped in the background of the noise and companies with secondary one.
- The chirping signal in the calculation frame converts to the wave rest frame and agrees well with the ideal sine wave function in spectrum.



- The best fitting of the sine function provides the time series of the wave amplitude and phase of the chirping signal.

Filtered Response Produces ‘WKB’ Expectation

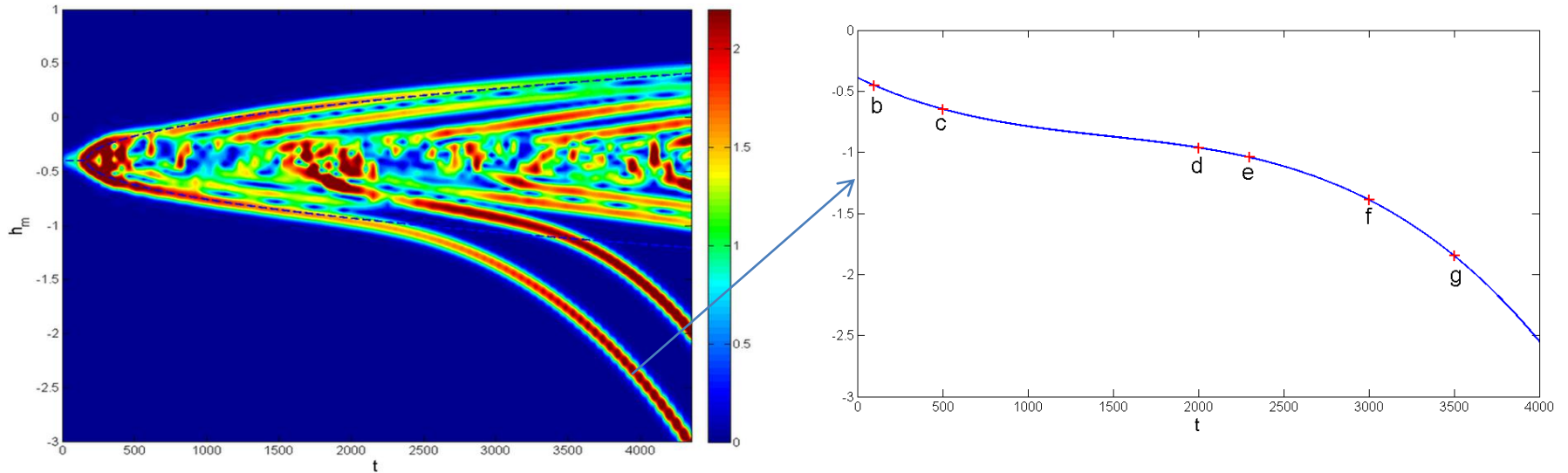
$$\text{ratio} = A_{\text{chirp}}/A_{\text{clump}}$$



$$A_{\text{clump}}(t) = \frac{-2i\eta_m \oint_{\text{clump}} f(\Omega, h_m) e^{i\theta} d\theta d\Omega}{\Delta_m - \sqrt{\frac{1+h_m}{1-h_m}}}$$

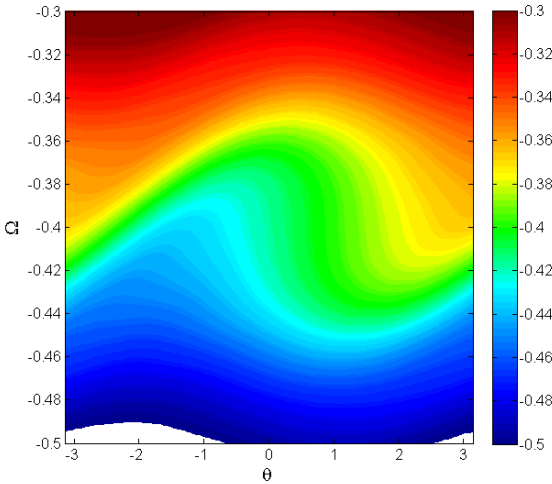
When the TAE wave chirps in the Alfvén gap, the ratio near 1 and 0 indicates the appropriateness of the adiabatic approximation, which shows the complex wave amplitude comparisons derived from the clump dynamics with the fast motions of trapped and pass-by energetic particles and the filtered chirping signal.

Dynamics of the Clump



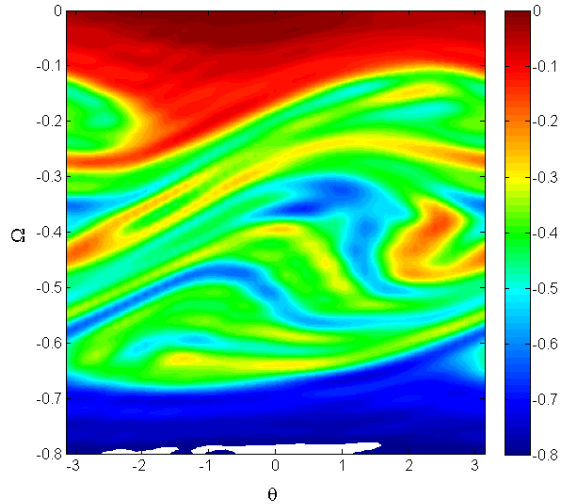
The sequence of snapshots (b)~(g) is caught along the curve of the downshifting chirped branch.

t=100



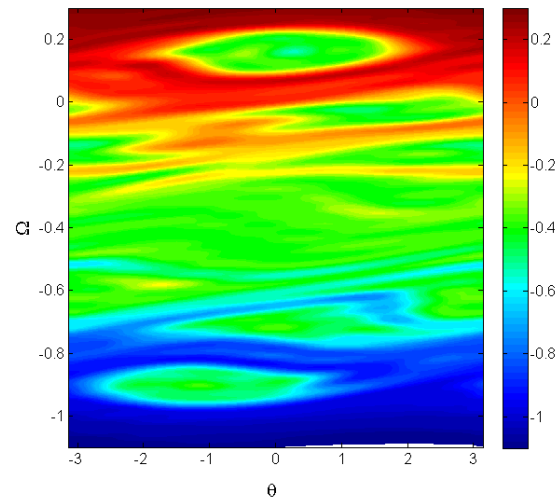
(b)

t=500



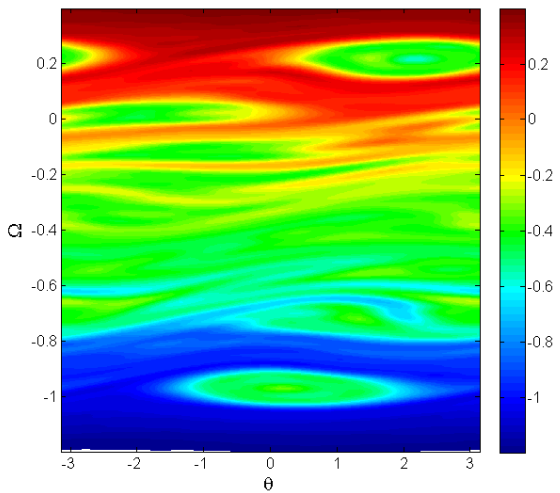
(c)

t=2000



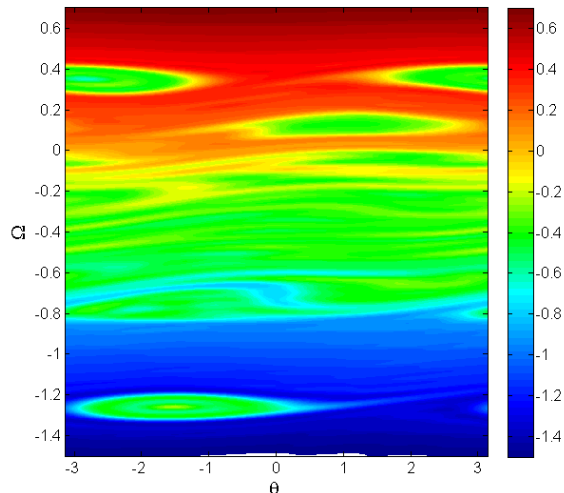
(d)

t=2300



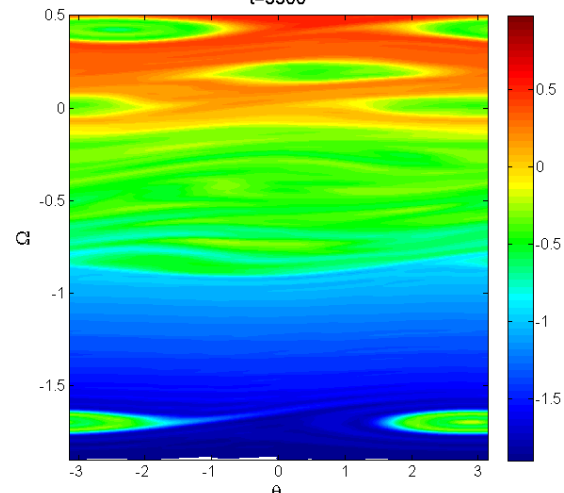
(e)

t=3000



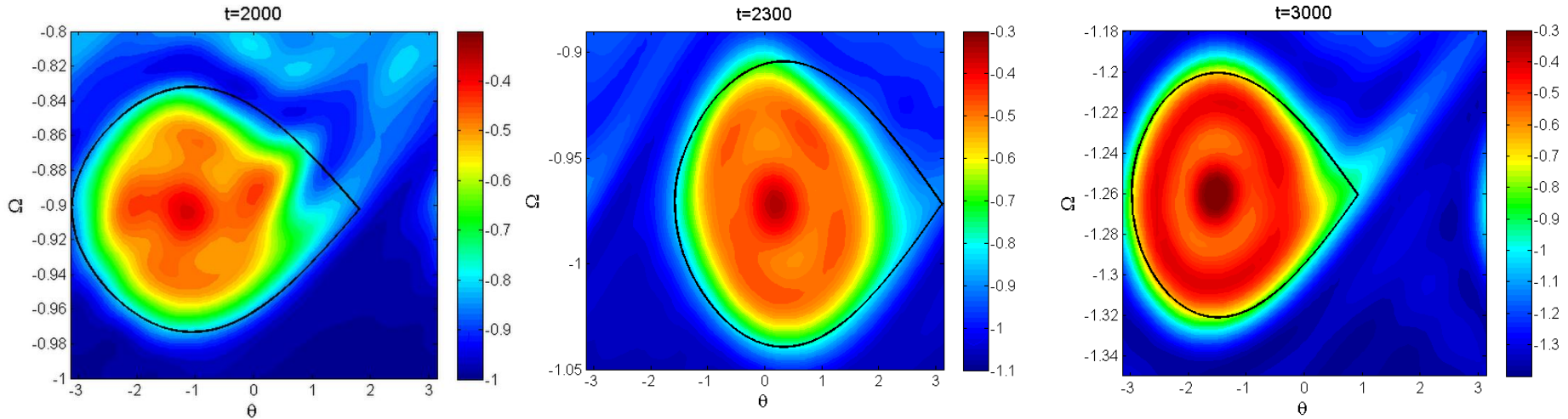
(f)

t=3500



(g)

Separatrix of Clump



The separatrix of clump is constructed from a Hamiltonian,

$$H = \frac{p^2}{2} - \omega_b^2 \cos q + \alpha q.$$

Both coordinate and momentum are defined as functions varying slowly with time,

$$q \equiv \theta - \omega_0 t - \int_0^t dt' \delta\omega(t'),$$

$$p \equiv \Omega - \omega_0 - \delta\omega(t).$$

Here ω_0 is the initial linear frequency and $\delta\omega$ indicates the instantaneous shift of frequency.

Conclusion

- Past analytic and previous simulations reproduced.
- Ability to move into frame of chirp structure
- Chirping Structures go into continuum at rate consistent with ‘WKB’ theory.
- The ‘WKB’ view description validates in accuracy when the clump propagates far from the gap-continuum boundary.
- The separatrix of the clump correlates with the chirping rate and amplitude of the chirped wave.

Thanks

FINIS

Track the chirping frequency

$$\begin{aligned}
 (\Delta_m - i)a(t) &= \int_0^t (J_0(t - \tau) - iJ_1(t - \tau))e^{i(\phi(t) - \phi(\tau))} a(\tau) d\tau \\
 &\quad + \frac{p}{\Delta_m - i}(J_0(t) - iJ_1(t))e^{i\phi(t)} - i4\pi\eta_m \tilde{f}_1(0, t), \\
 \frac{\partial \tilde{f}_n}{\partial t} + n \frac{\partial \tilde{f}_n}{\partial s} &= -\frac{is}{2}(a(t)\tilde{f}_{n-1} + 2\alpha\tilde{f}_n + a^*\tilde{f}_{n+1}) + \frac{1}{2}a(t)\delta(n-1)\delta(s),
 \end{aligned}$$

$$\theta(t = t_{lock}) = \theta_0 \text{ and } \Omega(t = t_{lock}) = \Omega_0, \quad a(t = t_{lock}) = p/(\Delta_m - i)^2$$

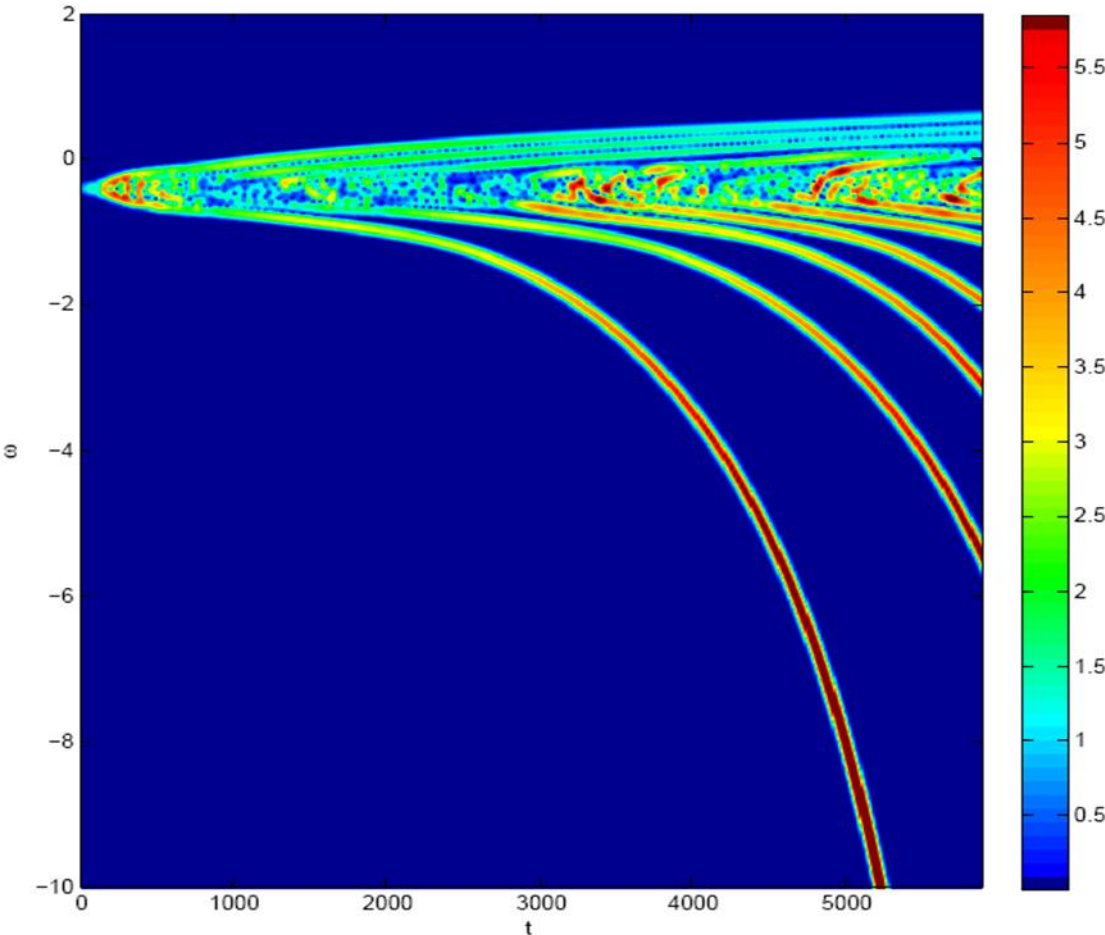
Where,

$$a(t) = A(t)e^{i(\theta - \theta_0)}, \quad \tilde{f}_n = \tilde{F}_n e^{in(\theta - \theta_0) - is(\Omega - \Omega_0)}$$

$$\frac{d\theta(t)}{dt} = h_{rex}(t) + i\gamma d.$$

$$\frac{dh_{rex}(t)}{dt} = \frac{h(T) - h_{rex}(t)}{\tau}$$

Future Work on Dramatic Chirping Events



- More realistic models for energetic particle current is being developed
- Include more ‘species’
- Can control be achieved for ‘good things’ e.g. burn control, channeling

Numerical Algorithm

- The Vlasov equation is integrated along the characteristic lines in the Fourier space s and n ,

$$\begin{aligned} \tilde{f}_n(s, t + \Delta t) = & \tilde{f}_n(s - n\Delta t, t) - \frac{i}{2} \int_0^{\Delta t} d\tau (s - n\tau) \\ & \cdot [a(t + \Delta t - \tau) \tilde{f}_{n-1}(s - n\tau, t + \Delta t - \tau) + 2\alpha \tilde{f}_n(s - n\tau, t + \Delta t - \tau) \\ & + a^*(t + \Delta t - \tau) \tilde{f}_{n+1}(s - n\tau, t + \Delta t - \tau)] \\ & + \frac{1}{2} a(t + \Delta t - s) \Pi\left(\frac{s}{\Delta t}\right) \delta_{n,1}. \end{aligned}$$

The TAE wave equation is a Volterra equation of the second kind.

$$\begin{aligned} (\Delta_m - i)a(t) = & \int_0^t (J_0(t - \tau) - iJ_1(t - \tau)) e^{i(\phi(t) - \phi(\tau))} a(\tau) d\tau \\ & + \frac{P}{\Delta_m - i} (J_0(t) - iJ_1(t)) e^{i\phi(t)} - i4\pi\eta_m \tilde{f}_1(0, t), \end{aligned}$$

The particle and wave coupling equations are solved in iterations until the convergence criterion satisfies.

Near Threshold Nonlinear Regime

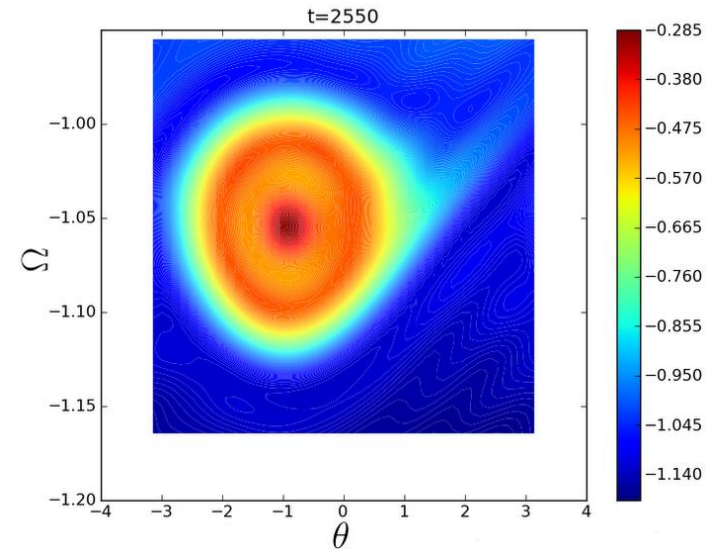
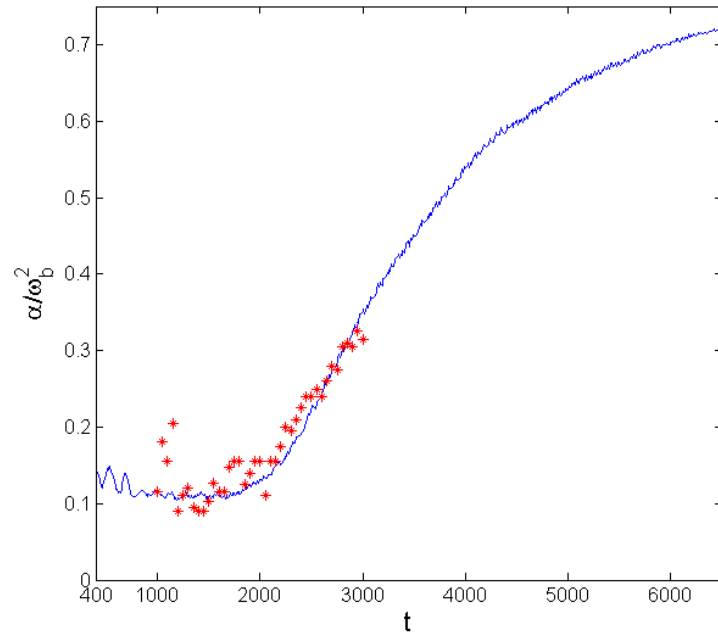
- The nonlinear response near the marginal stability

$$\gamma_L - \gamma_d \ll \gamma_L.$$

Where macroscopic plasma parameters evolve slowly compared to the instability growth time scale.

- Single-mode studied here simplifies the dynamics of particles to an action-angle pair (J, ϕ) .

Correlation of Clump Shape and Chirped Rate

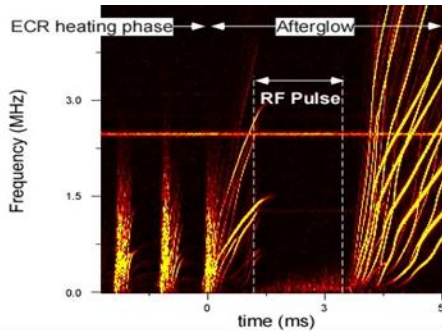


- The width of the clump reflects the chirping rate and amplitude of the TAE wave.

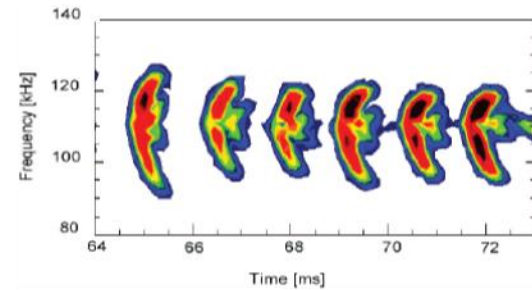
$$\frac{\alpha}{\omega_b^2} = \frac{1}{(2 + \Delta\theta^2 - 2\cos\Delta\theta - 2\Delta\theta\sin\Delta\theta)^{1/2}}$$

Examples of Chirping events

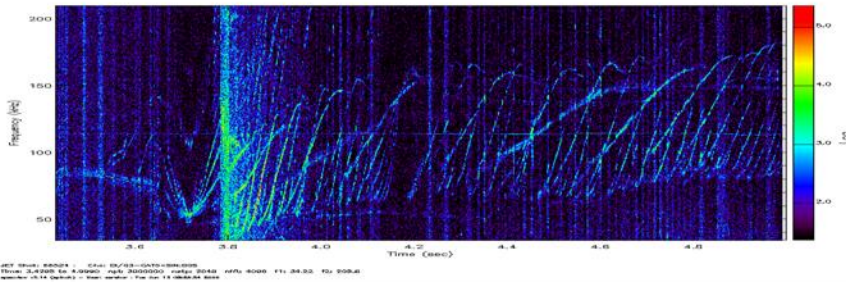
TERELLA



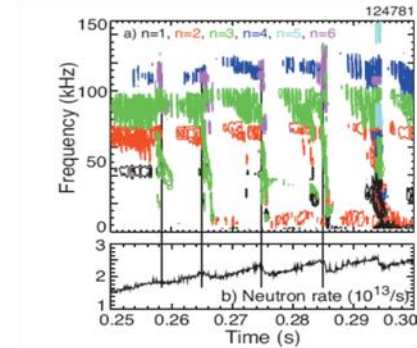
MAST



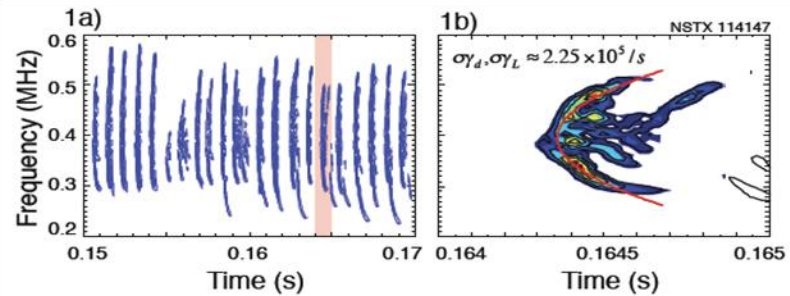
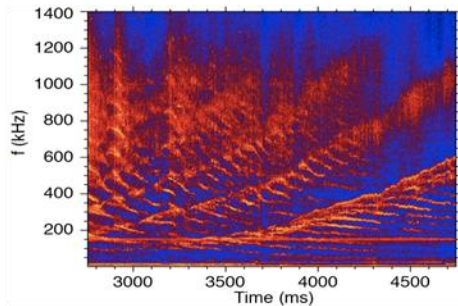
JET



NSTX



DIII-D



Chirping phenomena are extensively observed in the fusion related experiments.